

FIRST WALL AND BLANKET MODULE SAFETY ENHANCEMENT  
BY MATERIAL SELECTION AND DESIGN DECISION\*

B. J. Merrill

EG&G Idaho, Inc.  
Idaho Falls, Idaho

**MASTER**

Summary

A thermal/mechanical study has been performed which illustrates the behavior of a fusion reactor first wall and blanket module during a loss of coolant flow event. The relative safety advantages of various material and design options were determined.

A generalized first wall-blanket concept was developed to provide the flexibility to vary the structural material (stainless steel vs titanium), coolant (neutrium vs water), and breeder material (liquid lithium vs solid lithium aluminate). In addition, independent vs common first wall-blanket cooling and coupled adjacent module cooling design options were included in the study.

The comparative analyses were performed using a modified thermal analysis code to handle phase change problems.

The results indicate that:

- Pressurized water coolant and stainless steel structures provide the longest time for safety response to the transient for the systems studied,
- A liquid lithium breeder results in a level of afterheat for the system which can be removed by a tritium processing stream, whereas the afterheat of the solid breeder considered would require auxiliary cooling systems for the loss of coolant flow event.

In addition, the following design features were found to improve safety:

Design features that improve safety are:

- First wall designs of enhanced heat capacity,
- Independent first wall and blanket cooling systems,

- Adequate thermal coupling of the first wall and blanket structures,
- Thermal/fluids linking of adjacent blanket sectors.

Introduction

The safety concerns associated with flow disturbances in fusion reactor blankets stem from the possible mobilization of activated material or the failure of a given structure, precipitating additional system failures. A thermal/mechanical study has been performed to determine the behavior of a fusion blanket concept which has been subjected to a loss of coolant flow event.

The thermal response of the first wall-blanket structure to a loss of coolant flow event leads to two distinct results:

1. The time response of the structure while the plasma is still producing power, primarily a first wall effect.
2. The afterheat effects following a plasma termination that lead to an equilibrium maximum blanket temperature.

The results of this investigation illustrate the relative safety advantages obtained from selecting various combinations of cooling, structural, and breeding materials. To minimize the effects of the design configuration considered, a generalized blanket concept was developed that could accommodate a variety of coolant, structural, and breeding materials, while still retaining the same first wall and blanket configuration. The material combinations considered are listed by case number in Table 1.

The study has assumed a plasma termination at the time melting occurs at the first wall as the means to compare response times for the variables under study, since fusion reactor plasma termination systems are not well defined.

\*Work supported by the U.S. Department of Energy, Director of Research, Office of Fusion Energy, under DOE Contract No. DE-AC07-761001576.

**DISCLAIMER**

This book was prepared as an account of work sponsored by an agency of the United States Government. Neither the United States Government nor any agency thereof, nor any of their employees, makes any warranty, express or implied, or assumes any legal liability or responsibility for the accuracy, completeness, or usefulness of any information, apparatus, product, or process disclosed, or represents that its use would not infringe privately owned rights. Reference herein to any specific commercial product, process, or service by trade name, trademark, manufacturer, or otherwise, does not necessarily constitute or imply its endorsement, recommendation, or favoring by the United States Government or any agency thereof. The views and opinions of authors expressed herein do not necessarily state or reflect those of the United States Government or any agency thereof.

Fig

The flow coastdown for each case was calculated based on standard external water pump or helium circulator systems.

Material afterheat becomes the major safety concern following plasma quench. The ability to remove this energy without providing auxiliary systems is a desirable safety feature. As most of the proposed tritium extraction processes require recirculation and cooling of the process stream, this study investigated the ability of the tritium extraction system to remove the afterheat and prevent structural damage.

The helium cooled, stainless steel module with a liquid lithium breeder (Table 1) was selected as the base case. Based on comparisons with this case, conclusions were drawn as to the relative merit of the material selections of the remaining cases. Discussions of blanket design, analytical approach and modeling, and the results of the analyses are contained within the subsequent sections.

### Blanket Design

Figure 1 presents a schematic of the generalized blanket design. This design has received a preliminary design analysis that required the thermal, mechanical, and nuclear performance of this concept to be similar to current conceptual designs.<sup>(1,2,3,4)</sup> However, the development of a functional blanket concept was not an objective of this investigation.

The notable features of this design are the tubular first wall, the rectangular blanket modules, and the inlet/outlet blanket plenums. The coolant for the outer portion of the D-shaped blanket enters from the bottom of the torus. After traversing the first wall, the coolant enters the blanket inlet plenum. Coolant from this plenum flows radially through the blanket, collects in the outlet plenum, and exits at the bottom of the torus. Most of the cases considered required more blanket coolant flow than could be supplied at desirable pumping powers via the first wall; and as a consequence, a flow bypass was allowed between the inlet of the first wall and the blanket inlet plenum.

The tubular first wall was assumed to be attached to the inlet blanket plenum to readily facilitate removal. The blanket plenums are constructed of parallel plates that accommodate the imposed coolant pressure loads with the aid of slotted support grids. The plenum plates adjacent to the blanket have elliptical openings to corrugated W-shaped structures. These structures serve as the blanket coolant passages, and provide support for the breeding and reflecting materials. The wall thickness for each structure was determined by specific thermal/hydraulic requirements and the allowable stress guidelines of the ASME Section III pressure vessel code.<sup>(6)</sup>

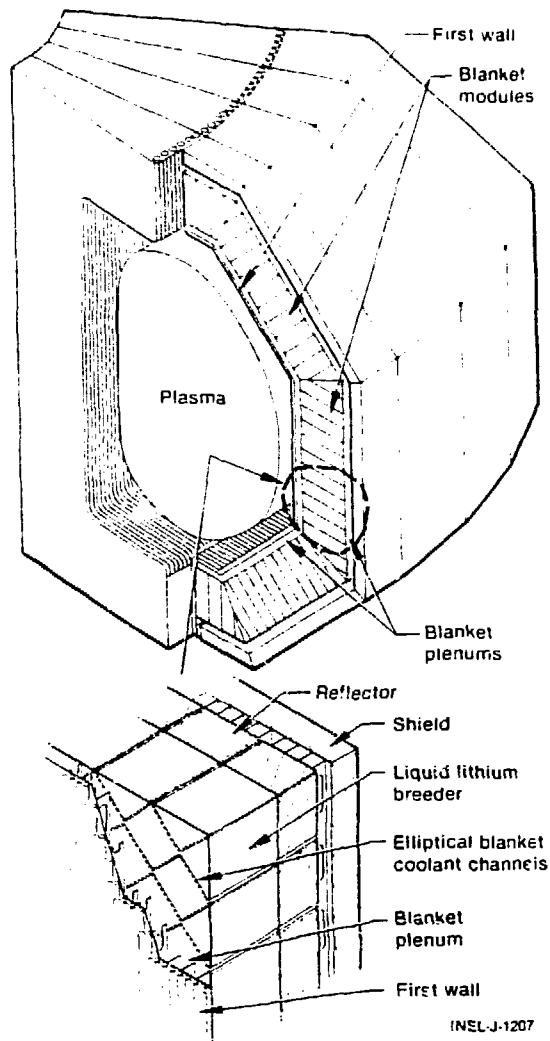


Figure 1: Schematic of a generalized fusion reactor blanket.

Table 2 contains some of the thermal/hydraulic constraints for each case, and Table 3 contains the radial widths of regions of the generalized design. To prevent excessive structural temperatures for the cases with a helium coolant, surface roughening of critical regions was assumed to give a doubling in convective surface coefficients at the expense of tripling the frictional losses.<sup>(7)</sup>

Five design alternatives were considered, which permit comparisons between two first wall materials, 316 stainless steel and titanium; between two breeding materials, liquid lithium and lithium aluminate; and between two coolants,

helium and water. The combinations of these choices into the five design cases are shown in Table 1.

### Analytical Approach and Modeling

The multidimensional heat conduction code, MITAS,<sup>(5)</sup> was used to model the response of the generalized blanket during the loss of coolant flow event. This computer program solves a set of finite differenced conduction equations that represent a model of the structure being considered. A change of material phase occurs for the water coolant. Thus, a modified thermal analyzer that handles this phenomenon was used in the MITAS program. The outer portion of the D-snaped blanket was modeled as five thermally isolated segments which were coupled only by fluid flow. Due to the design decision to have a detachable first wall structure, the primary mode of first wall to blanket heat transfer was by radiation.

The flow rate during coastdown history was obtained by equating the primary loop frictional force to the change in primary loop fluid momentum.<sup>(8)</sup>

Two-phase flow was approximated by constant friction multipliers<sup>(9)</sup> for water boiling during the flow coastdown. A detailed system response study would provide more accuracy. Such a systems modeling code is now under development at INEL.

Convective heat transfer coefficients were evaluated from one of several empirical relationships depending upon the coolant phase and flow regime. For all coolants, the Seider-Tate<sup>(10)</sup> and Dittus-Boelter<sup>(11)</sup> correlations were used for single phase laminar and turbulent flows, respectively. With water coolant, it is important to model boiling and dryout in a loss of coolant flow. A set of correlations that covered the range of boiling phenomena was employed. The Bergles and Rohsenow<sup>(12)</sup> and the Thom<sup>(13)</sup> correlations predicted nucleate boiling heat transfer. The MacBeth<sup>(14,15)</sup> correlations, the Bromley<sup>(16)</sup> correlations, and the correlation proposed by Miropolskii<sup>(17)</sup> were used for film boiling and dryout conditions.

The first wall neutron wall loading and surface heat flux were assumed to be  $4.0 \text{ Mw/m}^2$  and  $1.0 \text{ Mw/m}^2$ , respectively. The radial dependence of the neutron energy deposition was obtained from the ANISN<sup>(18)</sup> results shown in Figure 2. The volume ratios of the materials used to generate this information appears in Table 4. The DKR<sup>(19)</sup> code was used to calculate the afterheating of this design based on the ANISN predicted flux profiles for an operating period of two years. The predicted afterheating appears in Figures 3 and 4, respectively.

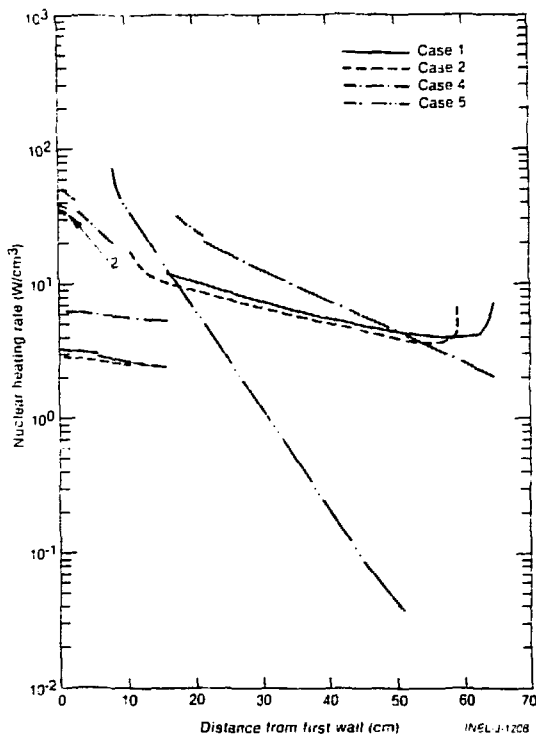


Figure 2. Volume averaged radial heating rate profiles for various cases.

### Results

The five material selection alternatives with some specific design variations were analyzed for loss of coolant flow until the first wall reached the melting point, as well as for some specific variations on some of the designs that are described below. The basic merit of each design for such a transient can be judged by the time that each design allows for safety system action, and the final steady state temperature after the transient is over. Table 5 summarizes these results. It can be seen that water cooling allows the longest time before the yield point or melting point is reached. Furthermore, equilibrium temperatures after the transient are lower with water than with helium coolant. The longest response time before reaching yield or melting, for Case 5, is a result of the thicker first wall tubes. The shortest response time, for Case 3, is a result of the thin titanium first wall. Solid breeding material causes higher equilibrium afterheat temperatures. Details of the transient scenarios are described below.

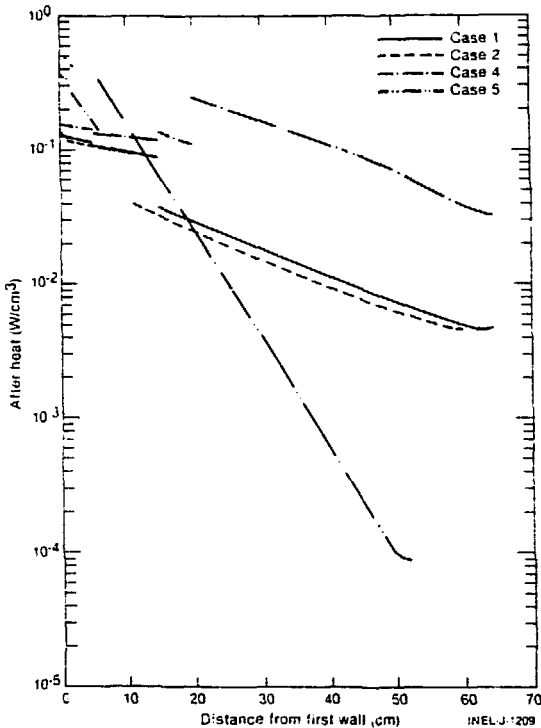


Figure 3. Volume averaged radial afterheat profiles at 30 sec for the various cases.

\*\*\*\*\*

### Discussion of Results

#### Case 1: Stainless Steel/Liquid Lithium/ Helium Cooled Design

The temperature response of the first wall was calculated for two loss of flow events: 1) the plasma burn continued and 2) the plasma burn is terminated concurrently with the loss of flow. Results are shown in Figures 5 and 6. Termination at loss of flow initiation shows the great improvement from safety system action which detects the flow loss.

In each case, a small, 180-K temperature change occurred in the blanket. With plasma burn continuing, the first wall reached 1060 K, corresponding to yielding, in 2.3 sec, and the melting point was reached in 8.1 sec, at which point the plasma burn was assumed to be

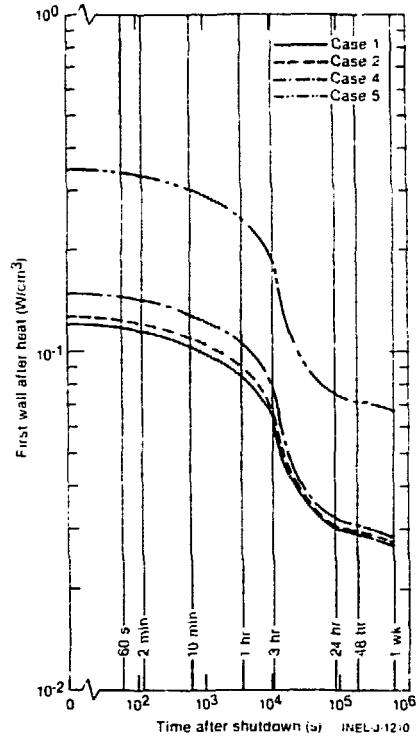


Figure 4. Volume averaged first wall after heat versus time for the various cases.

\*\*\*\*\*

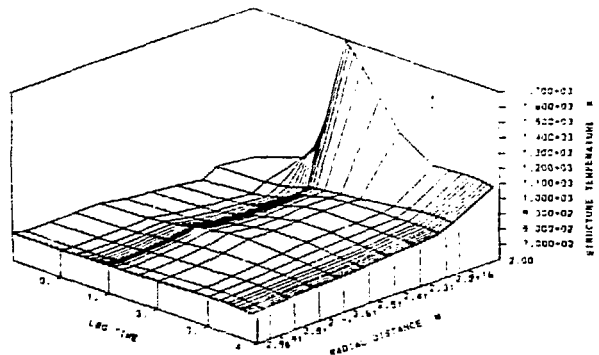


Figure 5. Structural radial temperature profile versus time (stainless steel/liquid lithium/helium cooled design, plasma burn termination coincident with first wall melting point).

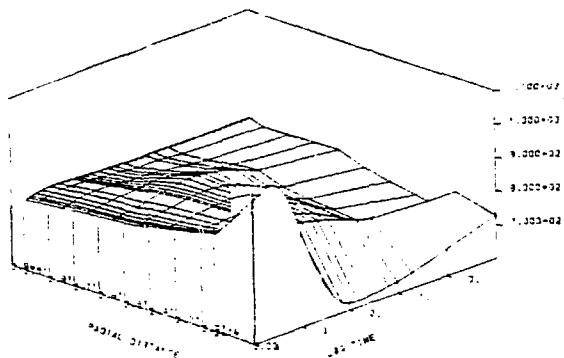


Figure 6. Structural radial temperature profile versus time for Case 1 B (stainless steel/liquid lithium/helium cooled design, plasma burn coincident with loss of coolant flow initiation).

\*\*\*\*\*

terminated. With early plasma burn termination, the flow remaining during the coastdown cooled the first wall to 620 K after 65 sec. In both cases, afterheat produced an equilibrium first wall temperature of 1050 K, essentially at yield. With early burn termination, the first wall rose to this temperature in 1.4 hours, one-half hour before the late-quench case cools to the same value.

Case 2: Stainless Steel/liquid Lithium/Water Cooled Firstwall/Helium Cooled Blanket Design

As shown in Figure 7, if both coolant systems fail, nucleate boiling of the water first wall coolant holds the first wall temperature for 3.0 sec. After 3.0 sec, a departure from nucleate boiling and a bulk dryout for the first wall coolant cause a sharp temperature rise. The first wall yield temperature was reached by 5.5 sec, and the inception of wall melt was reached at 9.0 sec. 3.1 sec later, the water rapidly quenches the wall, a transition to a second dryout occurs at 640 sec, and the temperature rises to an afterheat equilibrium of 890 K by 1.4 hrs. The noted contrast between these results and those of the helium-cooled base case are the faster first wall response for the water-cooled case once the heat transfer degradation began, and a final temperature below the yield point

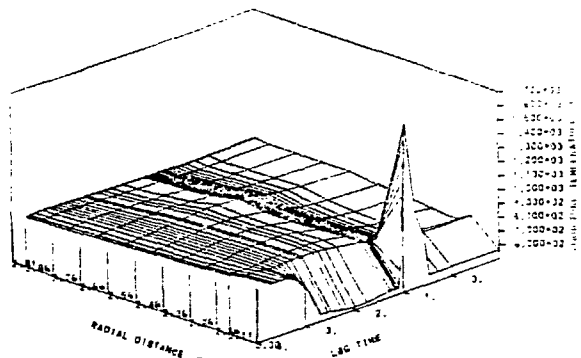


Figure 7. Structural radial temperature profile versus time for Case 2 (stainless steel/liquid lithium/water cooled first wall/helium cooled blanket design, loss of both cooling systems).

\*\*\*\*\*

value. These characteristics are the result of the smaller first wall tubing allowed by the water coolant.

With two coolant systems, it is unlikely that both systems would fail at the same time. Therefore, a calculation was performed where only the blanket coolant system was assumed to be lost. The results for such an event (Case 2B, Loss of Blanket Flow) appears in Figure 8 as maximum blanket structural temperature versus time. The structural yield temperature was surpassed by 65.0 sec, and melting occurred after 160.0 sec.

A preliminary investigation was also performed to determine the potential gain of thermal/fluids linking of adjacent sectors of the torus if the loss of coolant flow to a sector resulted from blockage. This linking was accomplished for the blanket by allowing for flow slots in the sector support structures in the region of the blanket inlet plenums. It was assumed that this design allowance would result in a flow redistribution among three adjacent sectors which would restore 67% of the initial flow in the blocked sector. The results of this case (Case 2c, Blockage of Blanket Flow) also appear in Figure 8 and can be compared with the blanket flow loss as representing a complete blockage. The yield temperature was not surpassed until 225 sec, and structural melt was averted by this simple design change.

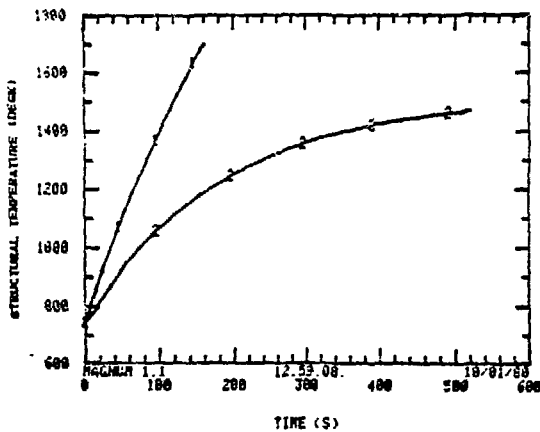


Figure 8. Maximum blanket structural temperature versus time for Case 2B and 2C (stainless steel/liquid lithium/water cooled first wall wall helium cooled blanket; upper curve: complete loss of blanket coolant; lower curve: flow redistribution allowed for blockage).

\*\*\*\*\*

Case 3: Titanium First Wall/Stainless Steel Blanket/Liquid Lithium/Helium Cooled Design

This case differs from the base case only in that a titanium first wall was used. As shown in Figure 9, the structural yield temperature of 1270 K was surpassed by 2.6 sec, only 0.2 sec sooner than the stainless first wall, but melting started at 5.0 sec, 3.1 sec sooner. Subsequent to plasma quench, the first wall temperature decayed to an afterheat equilibrium value of 926.0 K at 1.4 hrs. Contrary to the stainless first wall, the final first wall temperature was below the yield point. The rapid thermal response for this case was attributed to the thin tubes allowed by this alloy's high material strength and the low material heat capacity. The low final temperature was not only the result of the thin tubes, but also the low after-heating of this alloy.

Case 4: Stainless Steel/Lithium Aluminate/Helium Cooled Design

The impact of breeding material can be seen in the results of this case (Figure 10). The higher afterheat levels of the solid breeder resulted in higher final blanket temperatures.

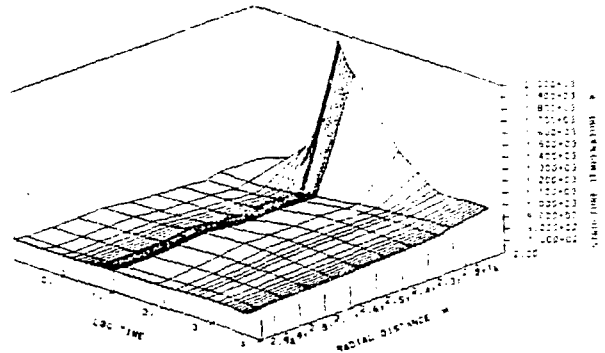


Figure 9. Structural radial temperature profile versus time for Case 3 (titanium first wall/stainless steel blanket/liquid lithium/helium cooled design).

\*\*\*\*\*

Less predominant aspects of this selection are the steady state radial temperature profile, the peaking at the front of the blanket, and the thermal decoupling of the reflector (note the slope change at 2.71 m). The first wall trends parallel to those of Case 1 up to about 130 sec, but subsequent to this time the temperature rise reflects the change in blanket composition. At approximately 2.8 hrs. the design reaches a thermal equilibrium with the afterheat. The resulting temperatures of the first wall, blanket inlet plenum, and the flow passages of the front of the blanket are still above the temperature for which the pressure produces stresses that are above yield.

Case 5: Stainless Steel/Lithium Aluminate/Water Cooled Design

This case with solid breeder and all-water cooling is shown in figure 11. The thicker first wall required to withstand the higher system pressure increased its heat capacity and slowed its response. Departure from nucleate boiling took 0.2 sec longer than in the water/helium coolant design. The first wall temperature peaked at 7 sec in film boiling near 1100 K, within 100 K of the yield point temperature. Then a change in heat transfer regime from film boiling to bulk dryout, possibly an artifact of the model, decreases the temperature. The first wall temperature then increases until structural melt occurs at 27.2 sec. The plasma

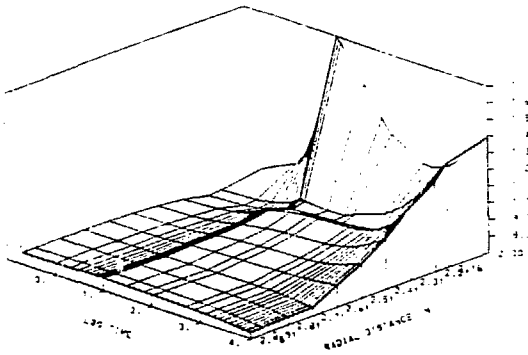


Figure 10. Structural radial temperature profile versus time for Case 4 (stainless steel/lithium aluminate/helium cooled design).

\*\*\*\*\*

burn was then terminated and the first wall experienced a rapid water quench. After approximately 0.9 hrs, it again entered bulk dryout, and by 0.9 hrs reached an afterheat equilibrium temperature of 1120.0 K. It can also be seen that prior to plasma burn termination, dryout of the blanket coolant caused structural temperatures at the front of the blanket to experience a rapid rise, followed by a prolonged quenching after the plasma was extinguished. The effect of first wall thickness can be very important when it is water cooled.

### Conclusions

Table 5 summarizes the results obtained for this case study of the loss of flow event. Based on these results, the first wall material selections which provide the longest time to respond prior to a structural failure are pressurized water and stainless steel. This was the result of the surface heat transfer characteristics and phase change of the water coolant, combined with the high heat capacity of stainless steel.

The first wall afterheat equilibrium temperature in three of the cases considered was above, or near, the value at which structural yield would occur. This situation could be remedied, for the design with the liquid lithium breeding material, by bonding the first wall to the blanket plenum, or depressurizing the primary system to eliminate the stress. The designs with lithium aluminate as a breeding material would

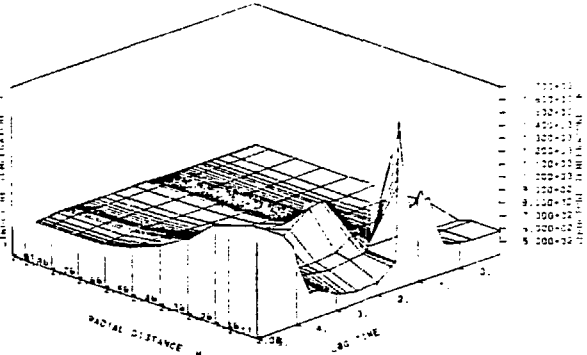


Figure 11. Structural radial temperature profile versus time for Case 5 (stainless steel/lithium aluminate/water cooled design).

\*\*\*\*\*

require either auxiliary cooling or system depressurization. Thus, the loss of coolant flow is an instance where liquid lithium blankets possess safety advantages over solid lithium blankets.

It was also concluded from the results of this study that the following design features have safety benefits:

- First wall designs of increased heat capacity,
- Independent first wall and blanket cooling systems,
- Thermal coupling of the first wall and blanket structures,
- Thermal/fluids linking of adjacent blanket sectors.

The following areas require additional analytic and design investigations:

- The afterheat of other solid breeding candidates,
- Flow redistribution between blanket sectors to aid in quantifying the advantages obtained during flow blockages,
- Safety enhancement of the first wall through composite structural materials and thermal/fluids linking,
- Total primary system response during flow disturbances.

### Acknowledgments

Acknowledgment is given to the contributions to this study made by T. S. Bohn for ANISN calculations, B. L. Harris for structural analysis, D. W. Nigg for DKR calculations, and, in particular, D. F. Holland for project guidance.

The submitted manuscript has been authored by a contractor of the U.S. Government under DOE

Contract No. DE-AC07-76ID01570. Accordingly, the U.S. Government retains a nonexclusive, royalty-free license to publish or reproduce the published form of this contribution, or allow others to do so, for U.S. Government purposes.

Work supported by the U.S. Department of Energy, Director Office of Energy Research, under DOE Contract No. DE-AC07-76ID01570.

TABLE 1. GENERAL BLANKET DESIGN MATERIAL SELECTIONS FOR THE LOSS OF COOLANT FLOW CASE STUDY

Case	First Wall		Blanket		
	Structure	Coolant	Breeder	Structure	Coolant
1	SS-316	Helium	Liquid Lithium	SS-316	Helium
2	SS-316	Water	Liquid Lithium	SS-316	Helium
3	Ti-6242	Helium	Liquid Lithium	SS-316	Helium
4	SS-316	Helium	LiAlO <sub>2</sub>	SS-316	Helium
5	SS-316	Water	LiAlO <sub>2</sub>	SS-316	Water

TABLE 2. DESIGN CRITERIA AND PARAMETERS

Parameter	Case 1	Case 2	Case 3	Case 4	Case 5
Maximum Structural Temperature (K)					
First wall	730.0	565.0	720.0	940.0	580.0
Blanket	773.0	773.0	773.0	773.0	614.0
Maximum Breeder Temperature (K)	1060.0	1060.0	1060.0	1100.0	1230.0
System Pressure (MPa)	5.5	5.5	5.5	5.5	13.2
Pumping Power, % of thermal output	4.5	1.5	4.5	4.5	.1
Coolant Outlet Temperature (K)					
First wall	550.0	535.0	540.0	550.0	535.0
Blanket	750.0	745.0	745.0	770.0	605.0
Coolant Temperature Rise (K)					
First wall	75.0	52.0	67.0	75.0	62.0
Blanket	225.0	270.0	225.0	250.0	132.0



TABLE 3. GENERAL BLANKET DESIGN REGION RADIAL WIDTHS (M)

Region	Case 1	Case 2	Case 3	Case 4	Case 5
First wall	0.053	0.007	0.052	0.053	0.007
Blanket Inlet Plenum	0.10	0.10	0.10	0.10	0.013
Multiplier	--	--	--	0.05	0.05
Blanket	0.50	0.50	0.50	0.45	0.45
Reflector	0.30	0.30	0.30	0.30	0.30
Blanket Outlet Plenum	0.10	0.10	0.10	0.10	0.012
Shield	0.20	0.20	0.20	0.20	0.20

TABLE 4. GENERALIZED BLANKET DESIGN MATERIAL VOLUME FRACTION (%)

Case	First Wall		Blanket		
	Structure	Coolant	Breeder	Structure	Coolant
1	8.2	70.3	93.3	2.3	4.4
2	3.0	70.5	93.3	2.3	4.4
3	5.2	73.3	93.3	2.3	4.4
4	8.2	70.3	72.2	9.6	18.2
5	18.6	60.0	61.8	18.4	19.8

TABLE 5. SUMMARY OF RESULTS

Case Number	Time to Exceed Structural Yield (sec)	Time to Exceed Structural Melt (sec)	First Wall Equilibrium Afterheating Temperature (K)
1. Stainless/He/Liq. Breeder	2.8	8.1	1056.0
2. Stainless/Water/Liq. Breeder	5.5	9.0	990.0
3. Titanium/He/Liq. Breeder	2.6	5.0	926.0
4. Stainless/He/Solid Breeder	2.8	8.0	1390.0
5. Stainless/Water/Solid Breeder	7.0	27.2	1120.0

## References

1. D. L. Smith, C. Trachsel et al., Fusion Reactor Blanket/Shield Design Study, ANL/FPP-79-1, July 1979.
2. J. S. Karbowski, Tokamak Blanket Design Program - Final Report, WFPS-TME-102, Westinghouse Electric Corporation, October 1978.
3. STARFIRE: A Commercial Tokamak Reactor, Interim Report, Argonne National Laboratory, October 1979.
4. R. W. Conn, "First Wall and Divertor Plate Material Selection in Fusion Reactors," Journal of Nuclear Material, 76 & 77, 1978, pp. 103-111.
5. G. M. Holmstead, "Martin Marietta Interactive Thermal Analysis System, Version 2.0 (MITAS II), User's Manual," EDTM-M-76-2, May 1976.
6. American Society of Mechanical Engineers, ASME Boiler and Pressure Vessel Code, Section III, "Nuclear Power Plant Components," Subsection NB, 1977 Edition, Spring 1979 Addenda.
7. Gas Cooled Fast Breeder Reactor Preliminary Safety Information Document, GA-10298, Amendment 3, April 1974, pp. 3.5-2.
8. W. E. Kastenburger, D. Okrent, G. C. Pomraning et al., Safety of Fusion Reactors, Final Report, PPG-342, October 1977.
9. R. C. Martinelli and D. B. Nelson, "Prediction of Pressure Drop During Forced Circulation Boiling Water," Trans, ASME, 70, 1948, p. 695.
10. F. N. Seider and G. E. Tate, Industrial Engineering Chemistry, 28, 1429, 1936.
11. F. W. Dittus and L. M. K. Boelter, "Heat Transfer in Automobile Radiators of the Tubular Type," Publications in Engineering, University of California, Berkeley, 2, pp. 443, (1930).
12. A. F. Bergles and W. M. Rohsenow, "The Determination of Forced Convection Surface Boiling Heat Transfer," Paper 63-HT-22, presented at the 6th National Heat Transfer Conference of the ASME-AIChE, Boston, August 11-14, 1963.
13. J. R. S. Thom, W. M. Walker, T. A. Fallon, G. F. S. Reising, "Boiling in Subcooled Water During Flow Up Heated Tubes or Annuli," Paper 6 presented at the Symposium on Boiling Heat Transfer in Steam Generating Units and Heat Exchanger, Manchester, September 15-16, 1965.
14. R. V. MacBeth, Burnout Analysis, Part 3, The Low Velocity Burnout Regime, AEEW-R 222, 1963.
15. B. Thompson and R. V. MacBeth, Boiling Water Heat Transfer--Burnout in Uniformly Heated Round Tubes: A Compilation of World Data with Accurate Correlations, AEEW-R, 356, 1964.
16. L. A. Bromley, N. R. LeRoy, J. A. Rebbers, "Heat Transfer in Forced Convection Film Boiling," Industrial Engineering Chemistry, 45, 12, 1953, pp. 2639-2645.
17. Z. L. Miropolskii, "Heat Transfer for Film Type Boiling of Water-Steam Mixtures Inside Steam Generating Tubes." Teploenergetika, No. 5, pp. 49-52, 1963.
18. W. W. Engle, Jr., A User's Manual for ANISN, K-1693, Oak Ridge Gaseous Diffusion Plant, 1967.
19. T. Y. Sung and W. F. Vogelsang, DKR: A Radioactivity Calculation Code for Fusion Reactors, UWFDM-170, Nuclear Engineering Department, University of Wisconsin, September 1976.